



UNITÉ DE RECHERCHE
INRIA-SOPHIA ANTIPOLIS

Institut National
de Recherche
en Informatique
et en Automatique

Domaine de Voluceau
Rocquencourt
B.P. 105
78153 Le Chesnay Cedex
France

Tél (1) 39 63 55 11

Rapports de Recherche

N° 657

**SIMPLE C^0 - APPROXIMATIONS
FOR THE COMPUTATION
OF INCOMPRESSIBLE FLOWS**

Roger PIERRE

Avril 1987

Simple C^0 -approximations for the computation of incompressible flows

Etude de quelques approximations C^0 pour la détermination d'écoulements incompressibles*

Roger PIERRE

Département de Mathématiques
Université Laval
Québec
G1K 7P4, Canada.

Résumé

Non étudions différentes procédures de régularisation permettant l'utilisation des éléments P1-P1 et Q1-Q1 pour la résolution du problème de Stokes à deux dimensions. Les résultats sont, dans le cas P1-P1, comparés à ceux obtenus à l'aide de l'élément Mini. Nous montrons qu'en fait, d'un certain point de vue, l'utilisation de cet élément est équivalente à une régularisation du type étudié. Finalement nous discutons de l'importance pratique de la condition de consistance et nous proposons une nouvelle formulation qui permet de la satisfaire même dans le cas P1-P1.

(*): Ce travail a été réalisé alors que l'auteur séjournait au centre de Sophia-Antipolis en tant que professeur invité du projet Sinus.

Simple C^0 -approximations for the computation of incompressible flows

Roger Pierre

Département de Math., Université Laval, Québec, G1K 7P4, Canada.

SUMMARY

We study various regularization procedures accomodating the P1-P1 and Q1-Q1 discretization of the 2D Stokes problem. The results are, in the P1-P1 case, compared with those obtained with a simple stable P1 element namely the Mini-element. It is shown that the use of the latter is in fact equivalent to a regularization method. Finally the practical importance of consistency is discussed and a new formulation is proposed to enforce that condition even in the P1-P1 case.

1. Introduction

Mixed finite element approximations of the Stokes problem have received a great deal of attention in the last few years. For the standard velocity-pressure formulation it was very early recognized that the approximations of the velocity field and of the pressure could not be chosen independantly if one wanted to get a stable scheme. In particular equal-order C^0 -interpolations are known to generate parasitic pressures that would require filtering. Mathematically speaking these elements do not satisfy the inf-sup condition of Brezzi and Babüska. On the other hand, since they are very attractive from the computational standpoint, people have been looking for alternate discrete formulations of the problem that would allow the use of the simplest of them, namely the P1-P1 or Q1-Q1 element.

One of the first such formulation was proposed by Brezzi and Pitkaräranta in [3]. There, they showed that their scheme was indeed stable but remarked that it was not consistent (in a sense to be precised later). More recently Hughes and al. generalized Brezzi and Pitkaräranta's idea in such a way as to insure consistency. Unfortunately their formulation reduces to the first mentionned in the P1-P1 case. In view of the practical interest of these low order elements it seems to be worthwhile to look for different ways of implementing their ideas in this context.

The purpose of this paper is twofold. First we want to compare the numerical behavior of these regularization procedures with the behavior of a low order element known to satisfy the inf-sup condition, namely the Mini element of Arnold, Brezzi and Fortin. Next we propose alternate formulations of Hughes's idea that retain consistency even for the P1-P1 element and give numerical evidence of the importance

of that notion.

An outline of the remainder of the paper follows: In Section 2 we review the variational formulation of the Stokes problem and its classical discrete counterpart giving some hints on the spurious pressures that may arise when solving it. The various regularization procedures are presented in Section 3 together with the notion of consistency. In Section 4 some remarks are made on the implementation problems, in particular on the treatment of boundary conditions in the Dirichlet case. Numerical results are discussed in Section 5 and conclusions drawn in Section 6.

2. Discretization of the Stokes problem

In this section we introduce the theoretical framework together with the necessary notation. We then recall some known facts about equal-order interpolation and present the Mini element.

2.1. Finite element formulation

The setting for our discussion will be the steady Stokes equations. We consider a polygonal domain Ω in two dimensions. The boundary will be denoted by Γ and the unit normal and tangent vectors along it by \underline{n} and $\underline{\tau}$ respectively. We present the problem in its classical variational form.

$$\begin{cases} \int_{\Omega} \nabla \underline{u} : \nabla \underline{v} \, d\underline{x} - \int_{\Omega} p \nabla \cdot \underline{v} \, d\underline{x} = \int_{\Omega} \underline{f} \cdot \underline{v} \, d\underline{x}, & \forall \underline{v} \in V, \\ \int_{\Omega} \nabla \cdot \underline{u} q \, d\underline{x} = 0, & \forall q \in L^2(\Omega). \end{cases} \quad (1)$$

Here the function space V is chosen in accordance with the prescribed boundary conditions. In order to discretize (1), we introduce finite element subspaces $V^h \subset V$ and $Q^h \subset L^2(\Omega)$ consisting of C^0 piecewise polynomials defined on a grid consisting either of triangles or of quadrilaterals.

We denote the grid by T_h (where h is the mesh size) and suppose that it satisfies the usual regularity conditions. In particular, if K is an arbitrary element of diameter h_K , we have

$$C_1 h_K^2 \leq \text{meas}(K) \leq C_2 h_K^2 \quad \text{and} \quad h \leq C_3 h_K,$$

where the C 's are positive constants. The discrete counterpart of (1) is then written:

$$\begin{cases} \int_{\Omega} \nabla \underline{u}^h : \nabla \underline{v}^h \, d\underline{x} - \int_{\Omega} p^h \nabla \cdot \underline{v}^h \, d\underline{x} = \int_{\Omega} \underline{f} \cdot \underline{v}^h \, d\underline{x}, & \forall \underline{v}^h \in V^h, \\ \int_{\Omega} \nabla \cdot \underline{u}^h q^h \, d\underline{x} = 0, & \forall q^h \in Q^h. \end{cases} \quad (2)$$

The problem is now to correctly choose the subspaces. Many combination of velocity and pressure approximations are known to lead to stable scheme, see for example [4]. Some are quite exotic, and in the C^0 case, few are easy to implement. On the contrary, approximations where one uses the same space for both variables offer obvious practical facilities. In this paper we will concentrate on the P1-P1 and Q1-Q1 elements, where the degrees of freedom are the values of the unknown at the vertices and where the polynomials are of the first degree either linear or bilinear.

2.2. The problem of the spurious pressures

As an illustration of the difficulties that one do encounter when using equal-order interpolation, we consider a specific exemple.

We want to solve the problem on the domain $\Omega = [0,1] \times [0,1]$ with boundary condition $\underline{u} = 0$ on Γ . For this, we use the P1-P1 element defined on the popular mesh illustrated in fig.1. Our aim is to show that, in this case, the system (2) is not well determined, because there exist non constant functions p^h for which

$$\int_{\Omega} p^h \nabla \cdot \underline{v}^h d\mathbf{x} = 0, \forall \underline{v}^h \in V^h. \quad (3)$$

To this end, we first restrict our attention to a shape function associated with an internal node. Its support Ω_0 is depicted in fig.1 where we indicated the appropriate numbering.

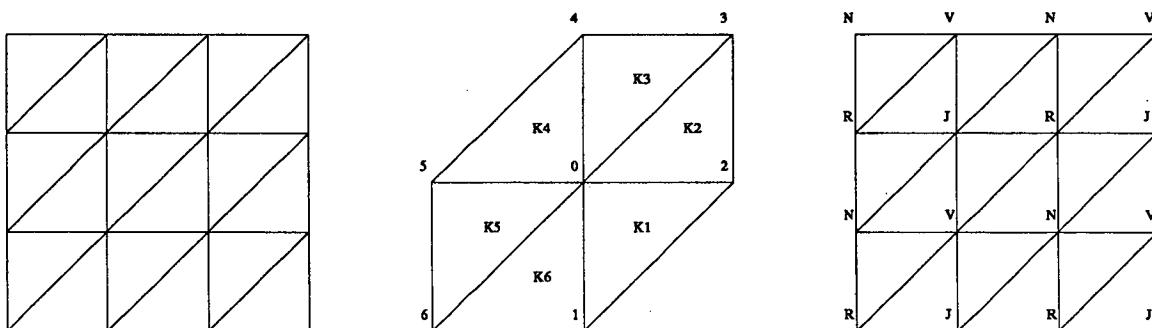


Fig 1: Left: Mesh, Center: Ω_0 , Right: Spurious pressures

Let ϕ_i denote the basis functions associated with the nodes involved. There are two velocity shape functions corresponding to node 0, namely $\underline{v}_{1,0} = (\phi_0, 0)$ and $\underline{v}_{2,0} = (0, \phi_0)$. It is clear that

$$\nabla \cdot \underline{v}_{1,0} = \begin{cases} -1/h, & \text{on } K_1 \text{ and } K_2, \\ 0, & \text{on } K_3 \text{ and } K_6, \\ 1/h, & \text{on } K_4 \text{ and } K_5. \end{cases}$$

Similarly

$$\nabla \cdot \underline{v}_{2,0} = \begin{cases} -1/h, & \text{on } K_3 \text{ and } K_4, \\ 0, & \text{on } K_2 \text{ and } K_5, \\ +1/h, & \text{on } K_6 \text{ and } K_1. \end{cases}$$

Thus, to find a pressure $p = \sum_{i=0}^6 p_i \phi_i$ defined on Ω_0 such that

$$\int_{\Omega_0} p \nabla \underline{v}_{i,0} \, d\underline{x} = 0, \quad i = 1, 2,$$

one has to solve the 2×4 linear system

$$\begin{cases} -p_1 - 2p_2 - p_3 + p_4 + 2p_5 + p_6 = 0 \\ 2p_1 + p_2 - p_3 - 2p_4 - p_5 + p_6 = 0. \end{cases} \quad (4)$$

It is easy to see that the general solution of (4) is of the form $(j, n, r, j + a, n - a, r + a)$, where the constants j, n, r, a are arbitrary. Now, to get a global solution of (3) we simply try to glue together the local solutions in such a way as to obtain a continuous function. Doing this, we are led to the pattern of fig.1. Such pressure solution, where the constants j, n, r, v are different will be termed *spurious*.

This example shows in particular, that the set of spurious pressures is much richer in the P1-P1 case than in the Q1-P0 one. Moreover, since this set is mesh-dependent the construction of specific filters appears to be trickier.

2.3. The Mini element

One way of getting around the problem of the spurious pressures is to enrich the space V^h by adding to it a set of functions with support restricted to each triangle. More precisely, to each triangle, we add a new degree of freedom given by the value of the velocity at the barycenter. Correspondingly, we add to V^h a bubble function defined by

$$\phi_4(\underline{x}) = \begin{cases} 27\phi_1(\underline{x})\phi_2(\underline{x})\phi_3(\underline{x}) & \text{if } \underline{x} \in K \\ 0 & \text{otherwise} \end{cases}$$

Here $\phi_i, i = 1, 3$ are the linear basis function associated with K . To see that this really does the trick, we consider a given triangle K and we successively set $\underline{v}^h = (\phi_4, 0)$ then $\underline{v}^h = (0, \phi_4)$ in (3). Upon integrating by parts, we are led to the equations

$$\begin{cases} \sum_{i=1}^3 p_i \int_K \frac{\partial \phi_i}{\partial x} \phi_4 \, d\underline{x} = 0, \\ \sum_{i=1}^3 p_i \int_K \frac{\partial \phi_i}{\partial y} \phi_4 \, d\underline{x} = 0. \end{cases}$$

Let B denote the matrix of the affine transformation that maps the reference element onto K . Some elementary calculations show that the above equations are equivalent to the linear system

$$B^{-t} \begin{pmatrix} p_2 \\ p_3 \end{pmatrix} = p_1 B^{-t} \begin{pmatrix} 1 \\ 1 \end{pmatrix}.$$

The solution of that system is simply $p_1 = p_2 = p_3$, which means, using continuity, that, with this new V^h , the only solutions of (3) are the constant functions.

The element corresponding to this construction, called the Mini element, was introduced by Arnold, Brezzi and Fortin in [1]. They showed, in fact, that this element satisfies the inf-sup condition (which does not follow from our elementary reasoning!). Unfortunately we will see that this element might not be rich enough, since in many tests, the pressure solution is plagued with small amplitude oscillations which look like a residual of the spurious pressures.

3. Stabilization by means of regularization

The idea of regularization is to modify the discrete equations instead of the approximation spaces. In this section we consider procedures based on an idea of Pitkäranta.

3.1. Regularization and consistency

In its simplest form, regularization amounts to add to the second equation in (2) a penalty-like term. But that term involves higher derivatives both of the discrete solution and of the shape functions, thus requiring more regularity on the approximation. The general form of regularized formulation that we consider is given by

$$\begin{cases} \int_{\Omega} \nabla \underline{u}^h : \nabla \underline{v}^h d\underline{x} - \int_{\Omega} p^h \nabla \cdot \underline{v}^h d\underline{x} = \int_{\Omega} \underline{f} \cdot \underline{v}^h d\underline{x}, \quad \forall \underline{v}^h \in V^h. \\ \int_{\Omega} \nabla \cdot \underline{u}^h q^h d\underline{x} + \sum_{K \in T_h} \epsilon_K(h) \left[\int_{\Omega} (\nabla p^h - \underline{f}) \cdot \nabla q^h d\underline{x} + C_h(\underline{u}^h, q^h) \right] = 0, \quad \forall q^h \in Q^h. \end{cases} \quad (5)$$

where the term $\sum (\epsilon_K(h) C_h(\underline{u}^h, q^h))$ is an approximation of

$$\int_{\Omega} (-\underline{\Delta} \underline{u}) \cdot \nabla q d\underline{x}. \quad (6)$$

The choice of C_h and of $\epsilon_K(h)$ will be made in accordance with the three following rules:

1. C_h and $\epsilon_K(h)$ should be such that the corresponding system (4) has a unique solution (up to a constant for the pressure in the Dirichlet case), so as to rule out the spurious

pressures.

2. The corresponding scheme should converge, and possibly preserve optimal rate of convergence when used with elements already known to be stable in the classical sense.

3. Formulation (4) should be *consistent*, that is to say that the corresponding method should be a *residual method*. More precisely, let (\underline{u}, p) be the solution of (2), then under suitable regularity assumption on Ω, \underline{f} and Γ , the system (5) should be satisfied with (\underline{u}, p) replaced by (\underline{u}^h, p^h) .

Remark 1

In the formulation of Brezzi and Pitkäranta, $C_h = 0$ and \underline{f} is set to zero in the second equation of (5). It is immediate to verify that, in that case, the first requirement is fulfilled as long as $\epsilon_K(h) > 0$. For the second, see [3]. As to the third rule, the effect of its violation will be studied in the next paragraph.

The formulation of Hughes and al. essentially corresponds to the case where

$$C_h(\underline{u}^h, q^h) = \int_K (-\underline{\Delta} \underline{u}^h) \cdot \nabla q^h \, d\underline{x}. \quad (7)$$

In particular for the P1-P1 approximation, $C_h = 0$. This is also true for the Q1-Q1 element on an orthogonal grid, since the term $\underline{\Delta} \underline{u}^h$ is zero in that case. Concerning the above rules, the reader may consult [5].

Remark 2

As to the choice of $\epsilon_K(h)$, theoretical results indicate that the right one is

$$\epsilon_K(h) = \alpha h^2 \quad (8)$$

and this is confirmed by experience. We will stick to that choice, but, now we're left with the problem of setting α correctly. From the theory, it turns out that α depends both on Ω and on the mesh (see [5]). From the practical point of view we will see that a good choice must take into account both the underlying spurious pressures and the boundary effect described below. In particular consistency seems to be an asset here.

3.2. On the relevance of consistency

The importance of that notion is not immediate for low order elements, at least from the point of view of the rate of convergence. In fact for both the P1-P1 and the Q1-Q1 element the error estimates, for the two formulations already considered, are identical. On the other end we will see that, when consistency is not satisfied, the

pressure solution of (5) do not behave very well near the boundary.

To illustrate this phenomenon, which is very similar to a boundary layer effect, we discuss the case $C_h = 0$ in (5) from a heuristic point of view.

Let's look at (5) as the discretized version of

$$\begin{cases} \int_{\Omega} \nabla \underline{u}^\epsilon : \nabla \underline{v} \, d\underline{x} - \int_{\Omega} p^\epsilon \nabla \cdot \underline{v} \, d\underline{x} = \int_{\Omega} \underline{f} \cdot \underline{v} \, d\underline{x}, \quad \forall \underline{v} \in V. \\ \int_{\Omega} \nabla \cdot \underline{u}^\epsilon q \, d\underline{x} + \epsilon \int_{\Omega} \nabla p^\epsilon \cdot \nabla q \, d\underline{x} = \epsilon \int_{\Omega} \underline{f} \cdot \nabla q \, d\underline{x}, \quad \forall q \in Q_0. \end{cases} \quad (9)$$

where Q_0 is a well chosen dense subspace of $L^2(\Omega)$. Using a standard reasoning and imposing some rather stringent regularity conditions on Ω, \underline{f} and Γ we see that the second equation in (9) corresponds to

$$\begin{cases} \nabla \cdot \underline{u}^\epsilon + \epsilon \Delta p^\epsilon = \epsilon \nabla \cdot \underline{f}, & \text{in } \Omega \\ \frac{\partial p^\epsilon}{\partial n} = \underline{f} \cdot \underline{n} & \text{on } \Gamma. \end{cases}$$

Under the same regularity assumptions, the first equation would be satisfied by the solution of (1) but not the second. In that case, the correct relation would be

$$\frac{\partial p}{\partial n} = \underline{f} \cdot \underline{n} + \underline{\Delta u} \cdot \underline{n} \quad \text{on } \Gamma.$$

We will exhibit simple analytic examples where this effect is clearly visible even if the rate of convergence is not affected.

3.3. Consistent formulation for low order approximation

To construct approximations of (6) which retain consistency and do not vanish in the low order case we use the following identity which is satisfied by any H^2 function. (We recall that we are working in two dimensions).

$$\underline{rot}(\underline{rot} \underline{u}) = -\underline{\Delta u} + \nabla(\nabla \cdot \underline{u})$$

where, for $\underline{u} = (u_1, u_2)$, $\underline{rot} \underline{u} = \frac{\partial u_2}{\partial x} - \frac{\partial u_1}{\partial y}$, whereas for any ϕ , $\underline{rot}(\phi) = (\frac{\partial \phi}{\partial y}, -\frac{\partial \phi}{\partial x})$. Using the fact that the solution u of (1) is divergence-free we get

$$\int_{\Omega} (-\underline{\Delta u}) \cdot \nabla q \, d\underline{x} = \int_{\Omega} \underline{rot}(\underline{rot} \underline{u}) \cdot \nabla q \, d\underline{x}.$$

On the other end integrating the right-hand side by parts we obtain

$$\int_{\Omega} (-\underline{\Delta u}) \cdot \nabla q \, d\underline{x} = \int_{\Gamma} \underline{rot} \underline{u} \cdot \nabla q \cdot \underline{\tau} \, d\sigma.$$

Of course, in the Q1-Q1 or in the P1-P1 case these formulas are not valid, since then, the elements of V^h are neither divergence-free nor in H^2 . But this suggests the following definitions

$$C_h^1(\underline{u}^h, q^h) = \int_K \underline{rot}(\underline{rot} \underline{u}^h) \cdot \nabla q^h \, d\underline{x} \quad (10)$$

$$C_h^2(\underline{u}^h, q^h) = \int_{\partial K \cap \Gamma} \underline{rot} \underline{u}^h \cdot \nabla q^h \cdot \underline{\tau} \, d\sigma. \quad (11)$$

It is rather easy to check that, the choice $C_h = C_h^1$ with the Q1-Q1 element lead to a consistent scheme. For the P1-P1 case, $C_h^1 = 0$ and we obtain no improvement. It is not the same for C_h^2 and it will turn out that its use with low-order elements gives rather good results for 2D Stokes problem. As to the verification that the corresponding scheme comply with the above stated rules, it will be done in [6], together with a complete error analysis.

3.4. The Mini element from the regularization standpoint

Before going to computational considerations, we would like to look at the Mini element under a new light.

The idea behind the addition of bubble functions, is that the corresponding velocity degree of freedom can be eliminated prior to assembly by using the so called "static condensation". We want to show that this process is nothing but a regularization in the sense presented above. For this, we observe that, when using Mini, every element of V^h can be written as

$$\underline{u}^h(\underline{x}) = \underline{u}_1^h(\underline{x}) + \sum_{K \in T_h} \phi_K(\underline{x}) \underline{u}_K,$$

where \underline{u}_1^h is a P1-approximation of \underline{u} defined on T_h , \underline{u}_K is the velocity degree of freedom attached to the barycenter of K , and ϕ_K the corresponding bubble function. Next, we remark that:

1. For each $\underline{u}^h \in V^h$ we have

$$\int_{\Omega} \nabla \underline{u}_1^h \cdot \nabla (\phi_K \underline{u}_K) \, d\underline{x} = 0.$$

2. For each $K \in T_h$

$$\int_{\Omega} \nabla (\phi_K \underline{u}_K) : \nabla (\phi_K \underline{u}_K) \, d\underline{x} = \left(\int_K \nabla \phi_K \cdot \nabla \phi_K \, d\underline{x} \right) \underline{u}_K = A_K \underline{u}_K$$

where $d_1 \leq A_K \leq d_2$ for some positive constants d_1, d_2 independent of h . (Use the regularity assumption on the mesh).

3. For every K_1, K_2 in T_h such that $K_1 \cap K_2 = \emptyset$,

$$\int_{\Omega} \nabla(\phi_{K_1} \underline{u}_{K_1}) : \nabla(\phi_{K_2} \underline{u}_{K_2}) d\underline{x} = 0.$$

As a consequence, the momentum equations corresponding to a vertex contains no degree of freedom related to a triangle barycenter, and conversely the momentum equations corresponding to such a barycenter contains no velocity degree of freedom apart from \underline{u}_K .

This simplifies the static condensation greatly. Indeed, let us consider a given K . Set $\underline{u}_K = (u_K^1, u_K^2)$ and $\underline{f} = (f_1, f_2)$. If we integrate the pressure term by part, the momentum equation corresponding to the barycenter can be written,

$$\begin{cases} A_K u_K^1 + \int_K \phi_K \frac{\partial p^h}{\partial x} d\underline{x} = \int_K f_1 \phi_K d\underline{x}, \\ A_K u_K^2 + \int_K \phi_K \frac{\partial p^h}{\partial y} d\underline{x} = \int_K f_2 \phi_K d\underline{x}. \end{cases} \quad (12)$$

Let's now look at an arbitrary continuity equation which we write

$$\int_{\Omega} \nabla \cdot \underline{u}_1^h q^h d\underline{x} + \sum_K \int_K \nabla \cdot (\phi_K \underline{u}_K) q^h d\underline{x} = 0.$$

Integrating the second term by part we get

$$\int_{\Omega} \nabla \cdot \underline{u}_1^h q^h d\underline{x} - \sum_K \underline{u}_K \cdot (\nabla q^h |_K) \int_K \phi_K d\underline{x} = 0.$$

We observe again that

$$\int_K \phi_K d\underline{x} = C_K h_K^2 \text{ with } d_3 \leq C_K \leq d_4$$

where d_3, d_4 are positive and independent of h_K . If we go back to (2), we see that we can eliminate the momentum equations corresponding to a barycenter. This will affect only the continuity equations. We use (12) to rewrite these under the form

$$\int_{\Omega} \nabla \cdot \underline{u}_1^h q^h d\underline{x} - \sum_K (C_K / A_K) h_K^2 \int_K (\underline{f} - \nabla p^h) \cdot \nabla q^h \phi_K d\underline{x} = 0. \quad (13)$$

It is now quite clear that the use of static condensation with the Mini element corresponds to a regularization procedure. That procedure differs from those proposed

in 4.1 because of the weight ϕ_K appearing in the last term. Otherwise we remark that this formulation is very similar to the one of Brezzi-Pitkäranta. In particular one may easily check that it is not consistent. In section 5 we will use (13) to further analyse the behaviour of that element.

For now, we notice that this equivalent formulation of the Mini element is not without interest from the computational standpoint. In fact one may very well implement the continuity equation in the *symmetric* form (13) and, if needed, recover the barycenter degree of freedom from (12). Here we will not perform this last step since we want to compare approximations obtained from identical subspaces.

4. Matrix formulation

From now on, we limit our attention to the case of Dirichlet boundary conditions, $\underline{u}|_{\Gamma} = \underline{g}$ where \underline{g} satisfies the flux condition

$$\int_{\Gamma} \underline{g} \cdot \underline{n} d\sigma = 0. \quad (14)$$

The domain under consideration is $\Omega = [0,1] \times [0,1]$, and the grids used for the Q1-Q1 and P1-P1 elements are shown in fig.2.

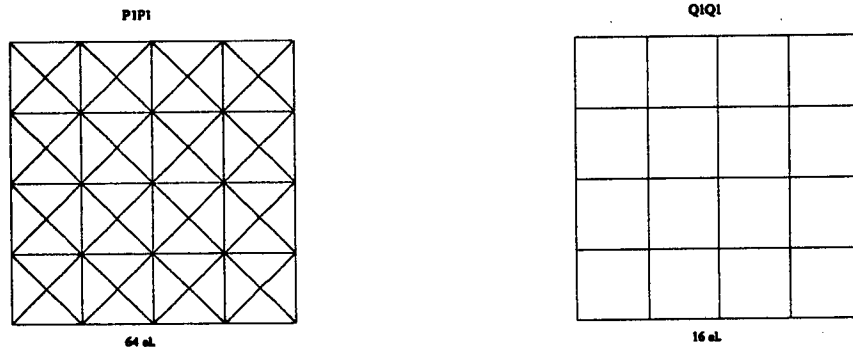


Fig.2: Grids

We will study three different formulations of the discrete problem in each case. We identify them in the following way.

- P1-P1:
- p1m1: formulation (4) with $C_h = 0$,
 - p1m2: formulation (4) with $C_h = C_h^2$,
 - p1m3: formulation (2) with the Mini element using static condensation.

- Q1-Q1: -q1m1:formulation (4) with $C_h = 0$,
 -q1m2:formulation (4) with $C_h = C_h^2$,
 -q1m3:formulation (4) with $C_h = C_h^1$.

In every cases,the matrix problem may be written as

$$\begin{pmatrix} A & -B^t \\ B + L & M \end{pmatrix} \begin{pmatrix} \underline{u}_d \\ p_d \end{pmatrix} = \begin{pmatrix} F \\ G \end{pmatrix}. \quad (15)$$

In (15), \underline{u}_d is the vector of unknown nodal velocity degrees of freedom and p_d the vector of nodal pressure degrees of freedom. We denote their dimensions by n_v and n_p respectively. The matrix A is the viscosity matrix, B the divergence Matrix, $-B^t$ the gradient matrix, M the *stabilization* matrix and L is the *consistency* matrix.

Remark 3

- When using equal-order interpolation together with formulation (4),the matrices A and M are constructed simultaneously from elementary Laplacian matrices.
- For plm1,plm3 and q1m1, $L = 0$, whereas for q1m3 the matrix L entails second order derivatives of the shape functions.
- For plm2 and q1m2, L entails only first order derivatives. Its determination at the element level is particularly simple on the cross grid (see fig.2), since each triangle has at most one side on the boundary which can be chosen to be the one joining vertex 1 to vertex 2.

The determination of F and G involves the implementation of boundary conditions. To illustrate this, we denote an arbitrary node by p and the corresponding basis function by ϕ_p . Next, we define a piecewise polynomial function $\underline{u}_0^h = (u_{0,1}^h, u_{0,2}^h)$ by

$$\underline{u}_0^h(p) = \begin{cases} \underline{g}(p) & \text{if } p \in \Gamma, \\ 0 & \text{otherwise} \end{cases}$$

For each node p the corresponding entries of F and G are then be given by

$$F_{p,k} = \int_{\Omega} f_k \phi_p \, d\underline{x} - \int_{\Omega} \nabla u_{0,k}^h \cdot \nabla \phi_p \, d\underline{x}, \quad k = 1, 2$$

$$G_p = \sum_K [\alpha h^2 (\int_K \underline{f} \cdot \nabla \phi_p \, d\underline{x} - C_h(\underline{u}_0^h, \phi_p))] - \int_{\Omega} \nabla \cdot \underline{u}_0^h \phi_p \, d\underline{x}.$$

Let $U = (1, \dots, 1)$ be an n_p -dimensional vector with entries all equal to 1. The compatibility condition corresponding to (14) is now written

$$G.U = 0 \quad (16)$$

By analogy with (14), we call (16) the discrete flux condition. With our choice of u_0^h this condition does not follow from (14). Indeed, using the definition of G_p , we see that

$$G.U = - \int_{\Omega} \nabla \cdot \underline{u}_0^h \, d\underline{x} = - \int_{\Gamma} \underline{u}_0^h \cdot \underline{n} \, d\sigma.$$

In fact, the right-hand side is, in the case under study, nothing but the approximation of $\int_{\Gamma} \underline{g} \cdot \underline{n} \, d\sigma$ given by the trapezoidal rule and therefore not automatically zero. When it is, we can fix the pressure at any node and solve.

Rather than doing that, we have used a penalty approach by adding to M a matrix λP where P is defined by

$$P_{i,j} = \int_{\Omega} \phi_i \phi_j \, d\underline{x}$$

and where λ is small as compared to αh^2 . This corresponds to the addition of a term $\lambda \int_{\Omega} p \, q \, d\underline{x}$ to the second equation in (1). The pressure solution of the penalized problem is now uniquely determined by (14) and must satisfy

$$\int_{\Omega} p \, d\underline{x} = 0.$$

On the other end, in this formulation, the discrete pressure is determined by the relation

$$\int_{\Omega} p^h \, d\underline{x} = -(1/\lambda) G.U,$$

and thus, when the discrete flux condition is satisfied, the arbitrary constant in the pressure is properly set.

Remark 4

We've favored the penalty approach for two reasons. First, in cases where the discrete flux condition was satisfied, we usually obtained better rate of convergence for the pressure than if we solved directly after fixing the pressure at one node.

Next, when (16) was violated, we observed that the velocities obtained by solving the penalty system were very good but that the pressure level was $O(1/\lambda)$, in accordance with the above remark. To get acceptable pressures we simply replaced p^h by

$$p^h - \frac{1}{\text{meas}(\Omega)} \int_{\Omega} p^h \, d\underline{x}.$$

This is a simple post-process and the resulting rate of convergence is as good as when (16) is true. However the boundary behaviour of the pressure is not as satisfactory, except perhaps when using C_h^2 . This way of getting around the discrete flux condition requires further analysis.

Remark 5

It can be shown (see [2]) that, for such a formulation as (5), the L^2 -penalty error is of order $O(\sqrt{\lambda})$. Since we expect $O(h^2)$ -precision for the velocities, it appears that a correct choice of λ would be $\lambda = O(h^4)$. That choice works but, for regular cases, the solution does not appear to be too sensitive to the value of λ .

5. Numerical results

To illustrate the various remarks made earlier, we consider three numerical tests, each one presenting its peculiarities. The first two have an academic character but were chosen because their analytic solutions are easy to manipulate. The last one is the classical lid-driven cavity problem which was already considered, in the same context, by Hughes and al. in [5].

5.1. Boundary behaviour of p

Let the force density \underline{f} in (1) be given by

$$\underline{f} = (-2(1-x), 2y).$$

If we impose obvious boundary conditions on $\Omega = [0, 1] \times [0, 1]$, the solution of the corresponding Stokes problem is given by

$$\underline{u} = (x^2, -2xy), \quad p = x^2 + y^2 + cte$$

The interest of this particular exemple lies in the following points:

- 1) The analytic solution is available thus permitting some quantitative error analysis.
- 2) The parasitic pressure associated with the p1m1 or the q1m1 formulation is easily obtained since \underline{f} is a conservative force field. In fact going back to 3.2, we get $p^\epsilon = x^2 + y^2 - 2x + cte$. In particular, while the level curves of p are circles centered at the origin, those of p^ϵ are circles centered at the point (1,0).
- 3) For the corresponding boundary conditions, the function $\underline{g.n}$ is piecewise linear, hence the discrete flux condition is satisfied.

We first present the results of the error analysis. For this we calculated the L^2 -error for both velocity and pressure. Those obtained by fixing the pressure at the origin at the value zero before solving the reduced system are denoted by ep1 and ev1. Those obtained by solving the penalty-system are denoted by ep2 and ev2. We made the following choice for the values of the parameters: $\alpha = 10^{-1}$, $\lambda = 10^{-6}$.

	ep1	ev1	ep2	ev2
p1m1	0.50 $h^{0.94}$	0.20 $h^{1.97}$	0.45 $h^{1.65}$	0.20 $h^{1.97}$
p1m2	1.50 $h^{0.99}$	0.10 $h^{2.05}$	0.97 $h^{1.76}$	0.10 $h^{2.04}$
p1m3	1.71 $h^{0.89}$	0.09 $h^{2.02}$	0.99 $h^{1.57}$	0.09 $h^{2.02}$
q1m1	0.16 $h^{0.87}$	0.21 $h^{2.00}$	0.20 $h^{1.67}$	0.20 $h^{1.99}$
q1m2	1.51 $h^{1.00}$	0.12 $h^{2.07}$	1.05 $h^{1.68}$	0.12 $h^{2.07}$
q1m3	1.48 $h^{1.00}$	0.12 $h^{2.06}$	0.99 $h^{1.67}$	0.12 $h^{2.07}$

Remark 6

We observe that the rate of convergence for the pressure is somewhat better with the penalty formulation. This might be attributed to the fact that, in the penalty approach, the so called hydrostatic pressure mode (see [7]) is not arbitrarily fixed, since its value is determined by the flux condition.

No conclusion should be drawn from the values of the multiplicative constants in the error terms. Indeed we have used the same value of α for the five methods, but we will see that this is not "optimal".

To give an exemple of the effect of the underlying spurious pressures, we solved the problem with $\alpha = 10^{-2}$ and the same value of λ as above. In Fig.3 we have the pressure fields on a mesh of 576 elements for q1m1, q1m2, q1m3 and p1m3. In every cases the oscillations are concentrated along the vertical parts of the boundary.

To get rid of the oscillations in the p1m3 case, we can either change λ or decrease the mesh size. We have done both and the results are shown at the bottom of Fig.3 where on the left, $\lambda = 10^{-3}$, while on the right we used $\lambda = 10^{-6}$ on a grid of 1600 elements. In the first case the error increases slightly and the oscillations are still present, in the second one the oscillations have not disappeared even though the error behaves nicely. For the other methods, the natural idea is to increase the value of α . In Fig.4, we present the results obtained for $\alpha = 10^{-1}$, $\alpha = 1$ and $\alpha = 10$ with q1m1 and q1m3 on the same mesh as the one used previously (*in that particular case*, the results of q1m2 are almost identical to those of q1m3). The effect of the increase is quite clear. Oscillations are disappearing, but for q1m1 the solution is distorted along the vertical walls. This is precisely the part of the boundary where

$$\frac{\partial p}{\partial n} \neq \frac{\partial p^\epsilon}{\partial n}$$

Already for $\alpha = 1$, it is seen that the problem comes from the normal derivative of p . It is the boundary layer effect described earlier and if one pushes α up to the value 10^7 the solution that one obtains is nothing but p^ϵ . Nevertheless the solution obtained for $\alpha = 10^{-1}$ is quite acceptable.

For the q1m3 case, α must be taken somewhat bigger to suppress the spurious components but the pressures are getting better and better. The important point is that even though its level increases, the velocity error remains acceptable, going from 0.00017 to 0.00019 when α varies from 10^{-1} to 10.

In Fig.5 we illustrate the results obtained with the P1P1 element. We can see that the above remarks concerning q1m1 apply to p1m1 apart from the fact that the boundary effect is more pronounced, even for small h . For p1m2, the situation is different. Even if we can eliminate the oscillations by choosing α bigger than one, we are left with a perturbation near the corners. This effect is very much reduced if we increase the number of elements but it is not totally eliminated. To what should this be attributed? It is not quite clear. It could be a consequence of the fact that, at the corners, the tangent to the boundary has a sharp discontinuity which affects the evaluation of the boundary integral. We have made no test to support this conjecture.

We can also use this exemple to show that the persistence of the oscillations in the pressure field produced by Mini is related to the size of the coefficients in the equivalent formulation (13). Indeed, if we implement the Mini element using that formulation, we can modify the regularizing term by multiplying the coefficient C_K/A_K by a constant β bigger than one. We stress the fact that this does not correspond to a simple modification of the bubble function. The results corresponding to $\beta = 10$ are shown in the bottom left of Fig.4 where one can see that the oscillations have been smoothed out. (This has been confirmed by other tests including one on the driven cavity discussed in 5.3). Unfortunately, this increases the velocity error by a factor of two. Since the resulting pressure field is very similar to that given by p1m1, and since implementing (13) is obviously more costly, it can be thought that the use of the Mini element is not really competitive.

To end the study of this exemple, we produce the velocity field obtained with p1m2 for $\alpha = 10^{-1}$, always on the same mesh. Those obtained by the other methods are almost undistinguishable.

5.2. A body force problem

This problem was suggested by Sani and al.[7]. If the appropriate (polynomial) body force is calculated from (1), the solution of the Stokes problem which vanishes on the boundary of the unit square, is

$$\begin{cases} u_1 = 2x^2(1-x)^2y(1-y)(1-2y) \\ u_2 = -2x(1-x)(1-2x)y^2(1-y)^2 \\ p = x^2 - y^2 \end{cases}$$

This solution is very smooth and, for this problem, even an element of doubtful quality such as the Q1P0 will converge at optimal rate. On the other end, the boundary conditions being homogeneous, we expect that their enforcement does

not create any problem either. In fact, whether we solved the system itself or its penalized version, the rates of convergence were $O(h^2)$ for the velocity and $O(h^{1.5})$ for the pressure.

We have restricted our attention to two methods, namely p1m1 and p1m2. As expected, in this case q1m1 is qualitatively equivalent to p1m1 while the same apply to q1m2 and q1m3 with respect to p1m2. The results given by p1m3 exhibit oscillations similar to those observed on the last exemple but of smaller amplitude.

In Fig.6 we present the pressure fields obtained by using both methods for $\alpha = 0.1, 1$ and 10 respectively. For p1m1, the best choice is $\alpha = 0.1$ and, for $\alpha \geq 1$ the boundary behaviour deteriorates, mainly near the origin where the pressure is too small. We computed the errors in each case: the pressure error takes the values $0.00148, 0.00852$ and 0.01414 while, for the velocity, we get $0.000187, 0.000573$ and 0.000964 . Hence as α goes from 1 to 10 the total error is roughly multiplied by 10 . On the other hand, for p1m2, the choice of α is not so crucial. The corresponding errors are $0.00110, 0.00130, 0.00308$ for the pressure and $0.000182, 0.000188$ and 0.000265 for the velocity, the total error being essentially multiplied by 3 . Thus *the practical advantage of consistancy* appears to be that the results are not so sensitive to the choice of the parameter.

In most of the tests that we've made the best value of α was between 0.1 and 1 for p1m1 or q1m1, although in some cases the boundary discrepancy was always visible even for small h . On the other hand for p1m2, q1m2 and q1m3 we usually had very acceptable results for α around 1 , mainly when taking h small enough to controll the corner effect observed on the exemple 5.1.

5.3. The lid-driven cavity

To conclude this section, we present the results of various tests on the popular lid-driven cavity problem. Unlike the preceeding exemple, this one is known to be very stiff because of irregular boundary conditions. Of course the discrete flux condition is satisfied here too.

We first treated the "flow through" case, i.e.

$$\underline{g} = \begin{cases} (1,0) & \text{if } y = 1 \\ (0,0) & \text{otherwise} \end{cases}$$

The resulting pressure fields are presented in fig.7 where we plotted the level curves corresponding to

$$p = \pm i, \quad i = 1, 11$$

All the results are quite acceptable except, maybe, those given by p1m3. We selected "optimal" values for α . In fact, for $\alpha \leq 0.01$, oscillations such as those appearing in the p1m3 case would be visible in the other ones too. This confirms that, as far as pressure calculations is concerned, Mini is not really competitive. In fig.8, we show the velocity fields computed with q1m1 and q1m2. Those obtained with the other

formulations are similar.

We repeated the calculations on a distorted mesh. As shown in fig.9, all the methods appear to be robust and continue to give acceptable results. We also used the same mesh for the exemple 5.1. There the situation was different. For p1m1, with $\alpha = 0.1$, the pressure field was everywhere polluted by oscillations. To suppress these oscillations we had to increase α but that aggravated the bad boundary behaviour. To the contrary, for $\alpha = 1.0$, the pressure field given by p1m2 was barely affected by the mesh perturbation. Here again, consistency seems to improve stability.

Finally, in fig.9, we illustrate the results given on a regular mesh, by p1m1 and p1m2, for the more difficult case of a contained flow, i.e.

$$\underline{g} = \begin{cases} (1,0) & \text{if } 0 < y < 1 \\ (0,0) & \text{otherwise} \end{cases}$$

For "optimal" α , the results are again very acceptable.

6. Conclusion

We have studied three different regularization procedures for the resolution of 2D Stokes problem. Their interest lies in the fact that they can be used with low equal-order C^0 -approximations such as P1-P1 or Q1-Q1.

In the P1-P1 case, we have compared the results given by two such formulations to those given by the Mini element. To this end, we have shown that, as far as pressure calculations were concerned, the use of that element was equivalent to a weighted regularization procedure similar to that of Brezzi and Pitkäranta. In particular, we were able to explain the persistence of small amplitude oscillations in the pressure field produced by Mini and to show that, as such, this element behaved worst then a regularized P1-P1.

From the computational standpoint, when used with equal-order element, regularized formulations are attractive but they require the choice of a parameter. Various tests indicate that this choice is easier if a *consistent* formulation is used. We studied two of these, one due to Hughes and al. which is also valid in the 3D context but which reduces to the Brezzi-Pitkäranta one in the P1-P1 case and one of our own which gives an improvement for both elements but which does not apply in 3D. Both methods behaved rather well with the parameter set to the value one and appear to be robust. On the other end, with the right α , inconsistent formulations can give very satisfactory results. Unfortunately they appear to be more sensitive to mesh perturbation.

An interesting quality of the Brezzi-Pitkäranta formulation is that it leads to a symmetric linear system, which is not the case with the other two. One way of retaining this advantage for consistent schemes would be to develop iterative procedures where the non-symmetric term could be sent to the right-hand side. Another

interesting point to investigate is the development of consistent formulations pertaining to the P1-P1 element in 3D. In the light of this work, this could lead to interesting new Stokes solvers.

ACKNOWLEDGEMENTS

Most of this work was realized during a stay of the author at the INRIA-center of Sophia-Antipolis. He would like to take this opportunity to thank Professor Alain Dervieux for his kind invitation and for providing very good computing facilities and a simulating scientific environment.

References

1. Arnold D.N., F.Brezzi and M.Fortin, A stable finite element for the Stokes equations, *to appear in Calcolo*.
2. Brezzi F. and M.Fortin, *book in preparation*.
3. Brezzi F. and J.Pitkäranta, On the stabilization of finite element approximations of the Stokes equations, In: W.Hackbush(ed.), Efficient solutions of elliptic systems, *Proceedings, Kiel, Jan. 1984. Notes on Numerical Fluid Mechanics, vol.10, pp 11-19, Vieweg, 1984*.
4. Fortin M. and A.Fortin, Experiments with several elements for viscous incompressible flows *Int.J.Numer.Methods in Fluids, vol.5,1985, 911-928*.
5. Hughes T.R.J., L.P.Franca, M.Balestra, Circumventing the Babūška-Brezzi condition: A stable Petrov-Galerkin Formulation of the Stokes Problem accomodating equal-order interpolation, *preprint, September 1985, to appear in Computer Methods in Applied Mechanics and engineering*.
6. Pierre R., Regularization procedures of mixed finite element approximations of the Stokes Problem, *INRIA report, in preparation*.
7. Sani R.L., R.M.Gresho, R.L.Lee and D.F.Griffiths, The cause and cure(?) of the spurious pressures generated by certain F.E.M. solutions of the incompressible Navier-Stokes equations, *Int.J.Numer. Methods in Fluids, vol 1, 1981, Part 1: 17,43, Part 2: 171-204*.

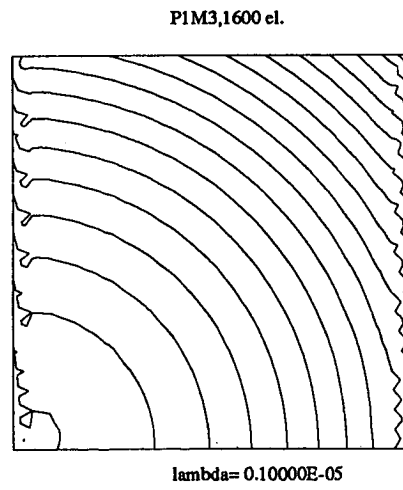
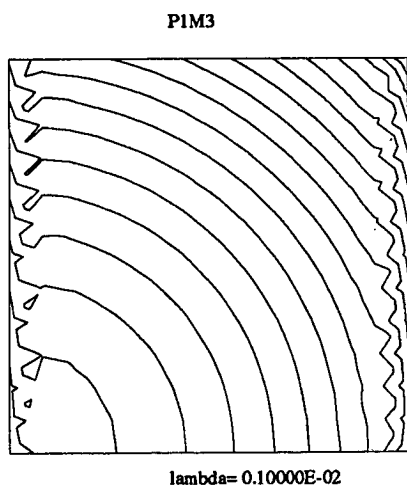
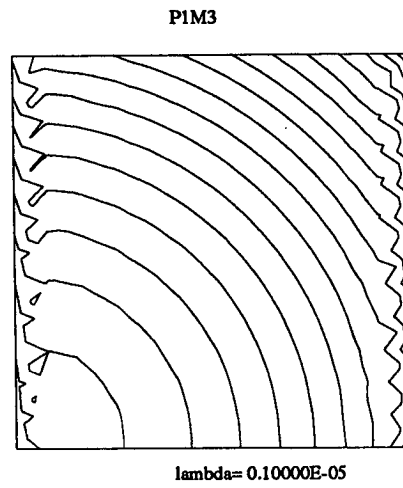
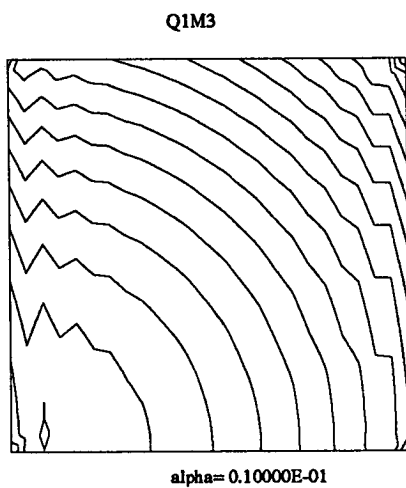
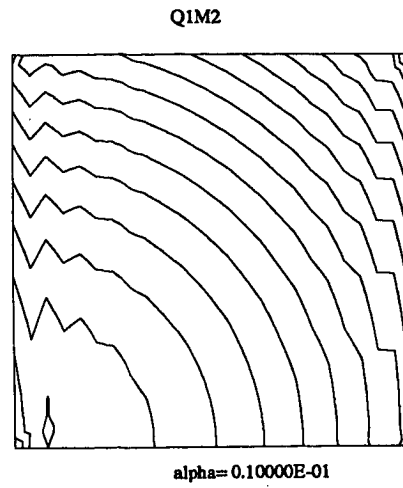
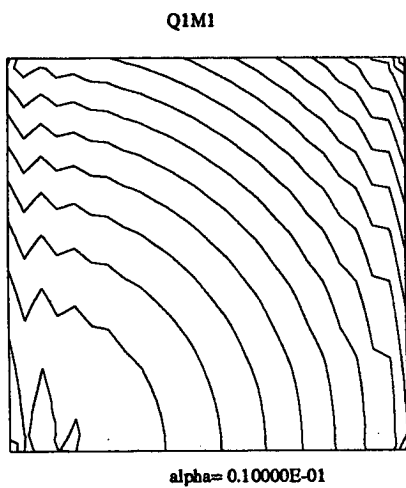


Fig 3: Residual spurious pressures

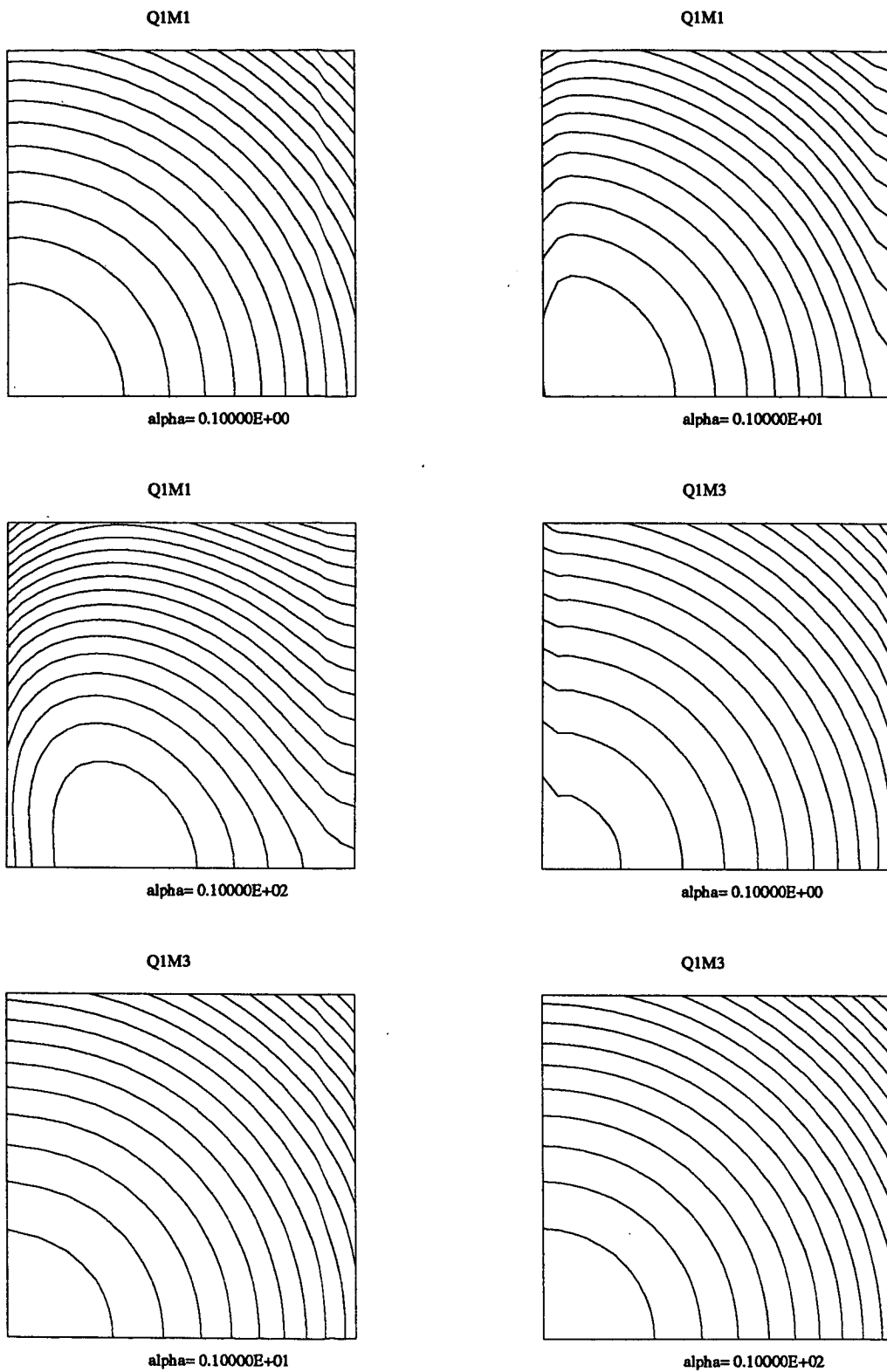


Fig 4: Boundary behaviour for Q1Q1

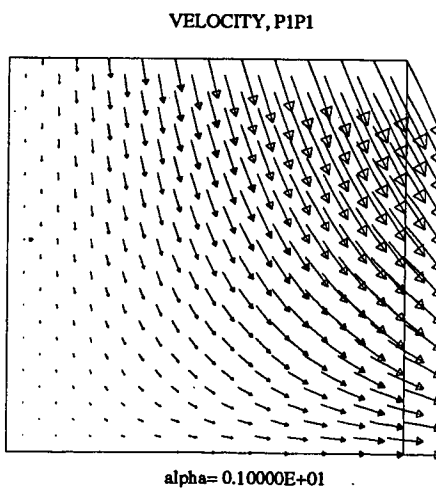
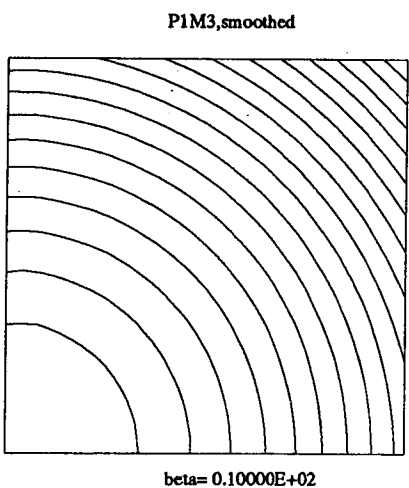
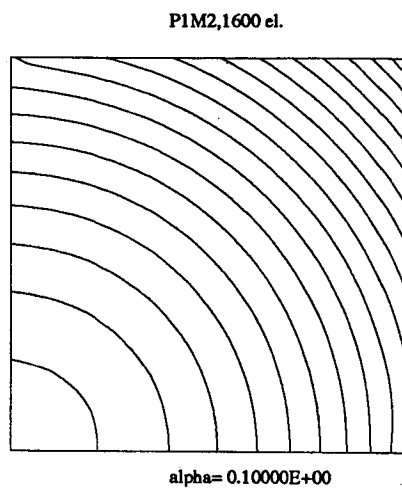
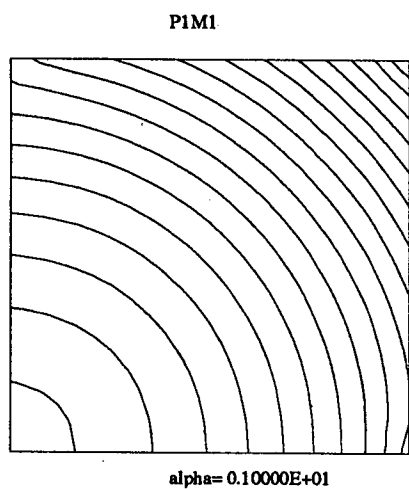
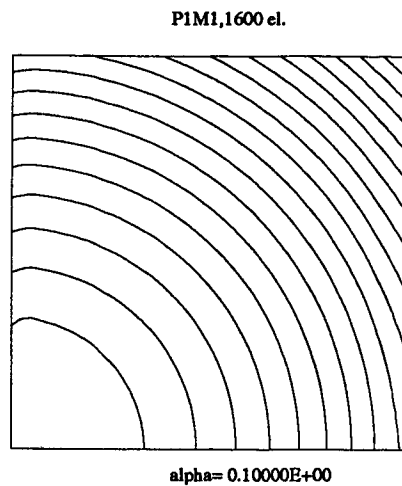
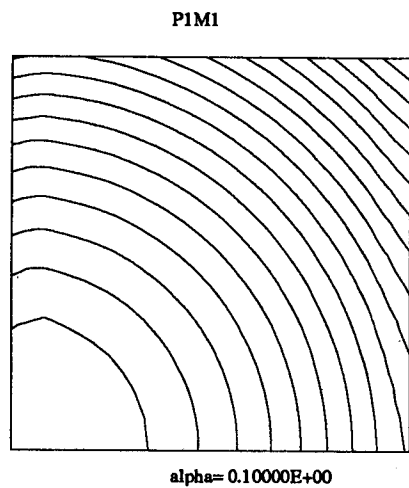


Fig 5: The P1P1 case

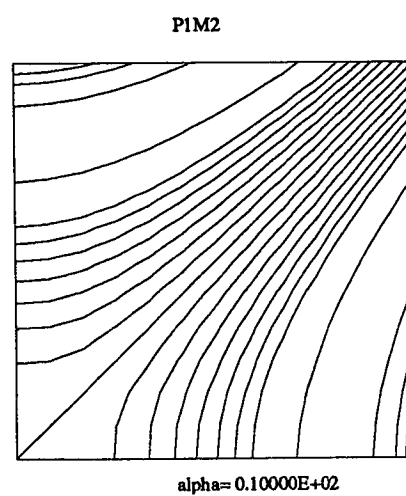
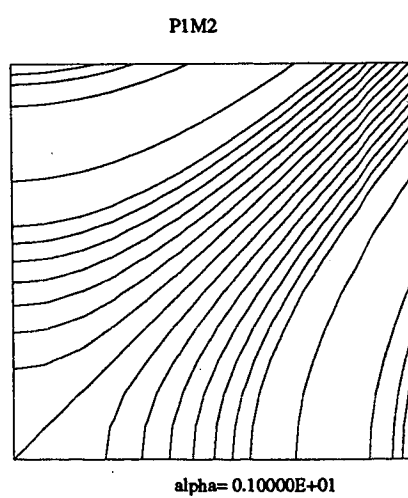
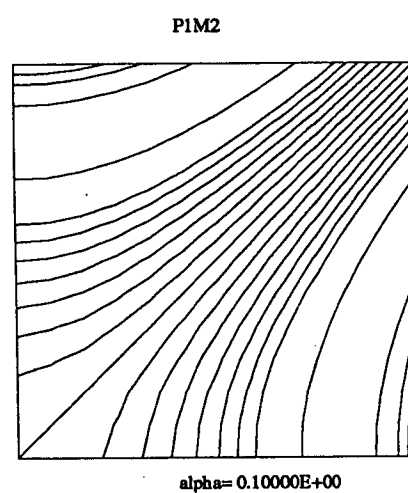
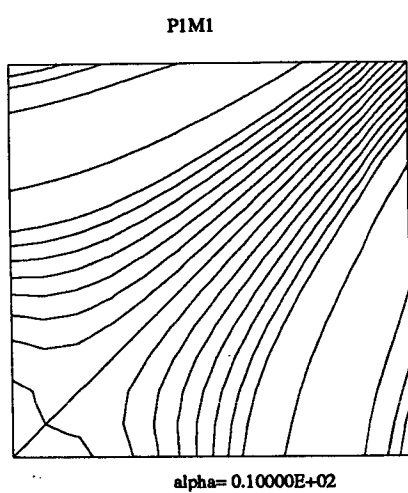
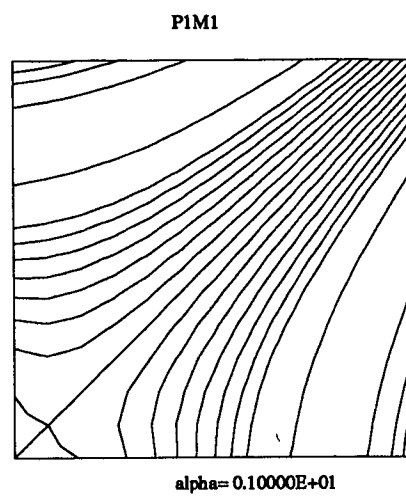
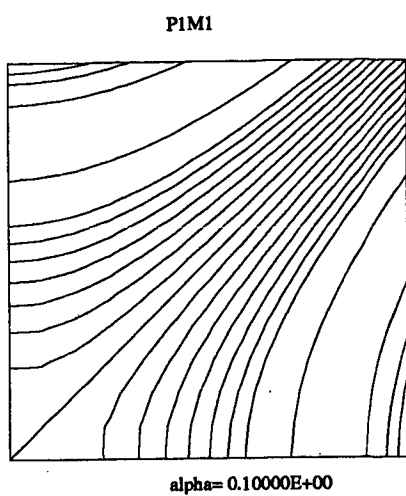


Fig 6: The body force problem

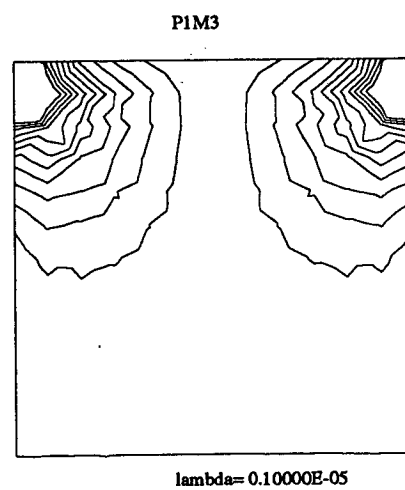
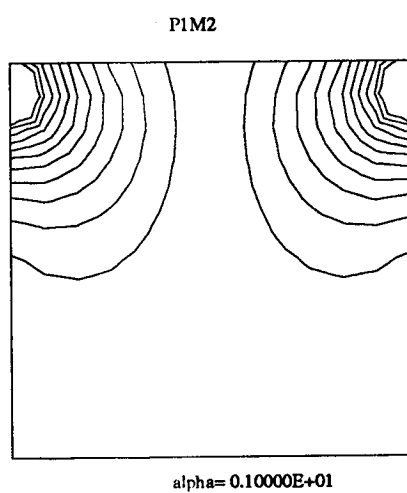
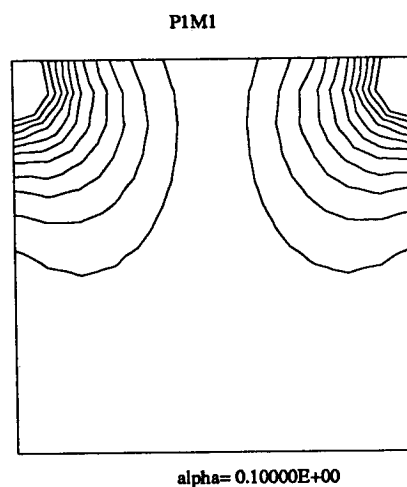
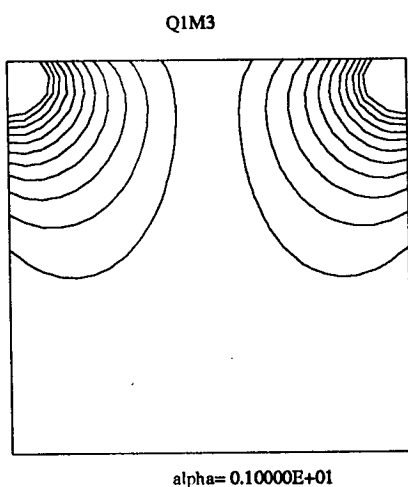
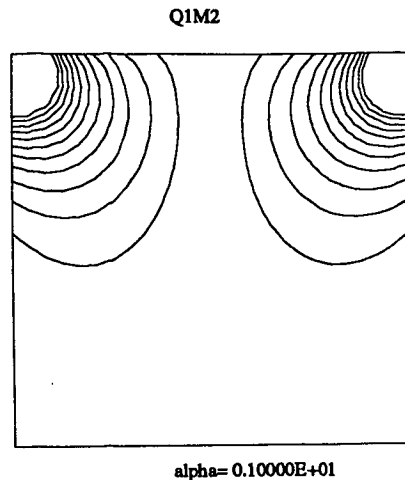
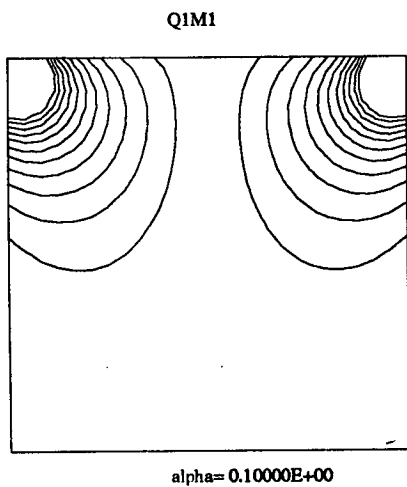


Fig 7: Cavity: "Flow through"

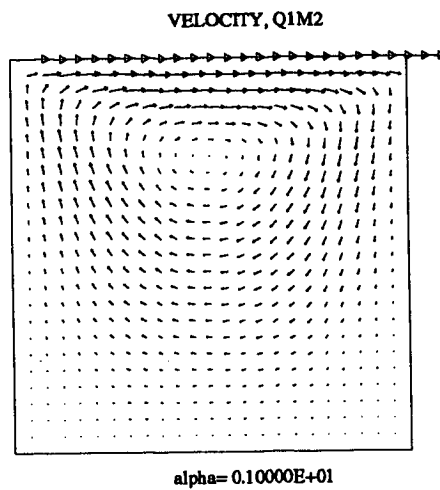
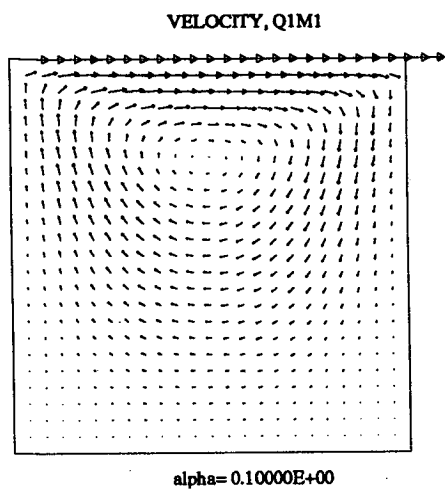


Fig 8: Cavity:"flow through"

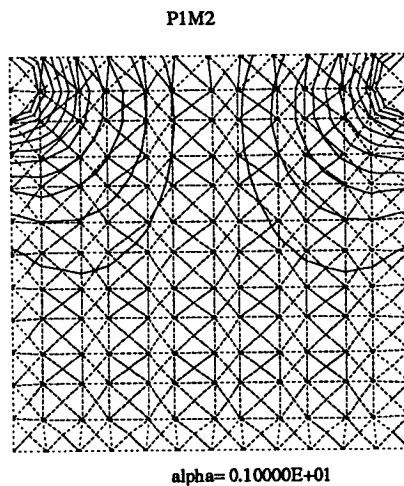
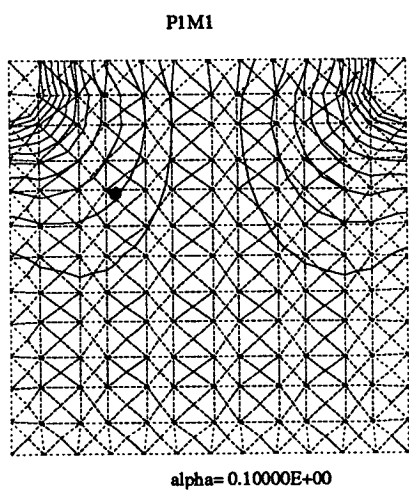


Fig 9: Cavity:ditto,distorted mesh

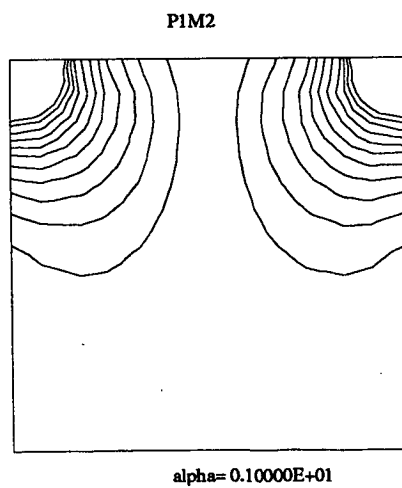
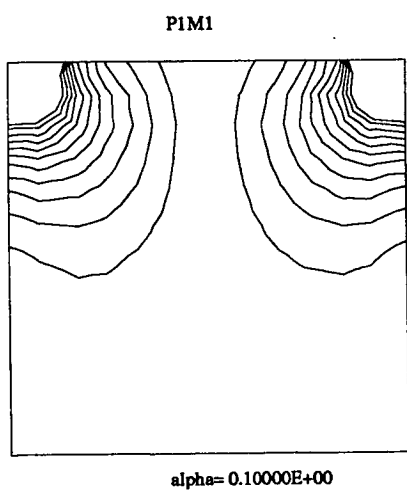


Fig 10: Cavity:"contained flow"

